J Electroceram (2006) 16:277–282
DOI 10.1007/s10832-006-9864-6

Dielectric anomalies of $Pb_{0.7}La_{0.2}TiO_3$-based perovskite

Hwee Ping Soon · John Wang

Abstract Dielectric transitions from normal ferroelectric to relaxor-like and then to quantum paraelectric-like behaviour were observed by substituting 10 to 60% of Ca^{2+} for Pb^{2+} into *A*-site of $Pb_{0.7}La_{0.2}TiO_3$ with the required stoichiometry of $Pb_{0.7(1-x)}Ca_{0.7x}La_{0.2}TiO_3$ (PCLT). The quantum ferroelectric relation that commonly applies to $SrTiO_3$-based perovskites, $T_{max}\alpha(X - X_c)^{1/2}$, fails to describe the observed dielectric anomalies in PCLT, whereby the transition temperature vanishes with a finite slope. Quantum ferroelectric behaviour that exhibits a sharp dielectric peak but violates the Curie-Weiss law was not observed throughout the composition range studied. Unlike the typical quantum paraelectric $SrTiO_3$, the quantum paraelectric-like behaviour observed for PCLT with $x = 0.55$ and 0.60 exhibit negative transition temperatures, as shown by the fittings to both the Curie-Weiss and Barrett's relations. Thermal hysteresis was surprisingly observed in substituted PCLT with $x = 0.30$ and 0.40 that exhibit frequency dispersive relaxation. To establish a correlation between the dielectric anomalies and structural parameters, analyses on global and local perovskite lattices were carried out using X-ray diffraction technique and micro-Raman spectroscopy.

Keywords Ferroelectric · Relaxor · Quantum paraelectric

1 Introduction

The ferroelectric behaviour of $PbTiO_3$ is largely affected by the types and concentration of defects and cation substitution, as well as the externally applied bias and hydrostatic pressure. As has been reported by Cohen [1], this is due to the delicate balance between the long-range Coulomb forces that favour the ferroelectric state and the short-range repulsions that favour the non-polar cubic state. According to the first principle calculations, the ferroelectric instability is manifested by the *d*-hybridization between the unoccupied 3*d* state of Ti and its neighbouring O, which acts to soften the Ti-O repulsion [1, 2]. Indeed, the dielectric transition from ferroelectric to relaxor is commonly triggered by *B*-site substitution in the perovskite structure, which directly modulates the nature of Ti-O hybridization. Although *d*-hybridization is the origin of ferroelectricity, lattice distortions in *A*-site of a perovskite lattice also play an important role in determining the average structure and the ferroelectric properties. This is particularly so due to the 12-fold symmetry of oxygen nearest-neighbour shell for *A*-site cation in contrast to that broken one for *B*-site [3]. In general, *A*-site substitution modulates the ferroelectric transition by affecting the ferroelastic strains, which couples with the lattice distortions of the perovskite lattices, and the nature of Ti-O hybridization. As had been indicated by extensive investigation into *A*-site chemical substitutions, such as Li^+-doped $KTaO_3$ and Ca^{2+}-doped $SrTiO_3$, dielectric transitions from quantum paraelectric to quantum ferroelectric and then to relaxor were resulted by an increasing level of substitution [4–7]. These interesting phenomena have been addressed as the impurity-induced ferroelectricity or polar-cluster effect, where the dipolar nano/micro-regions are induced by the off-centered impurities or their corresponding defect associations with high polarizability [8].

As suggested by Hennings [9], La^{3+} ($r = 1.032$ Å) can replace Pb^{2+} ($r = 1.19$ Å) rather than Ti^{4+} ($r = 0.605$ Å) by creating *A*-site vacancy in the $Pb_{0.7}La_{0.2}TiO_3$ perovskite lattice ($c/a \sim 1.02$), leading to a strain field in Ti-O octahedral, which gives rise to normal ferroelectric that undergoes

H. P. Soon · J. Wang (✉)
Department of Materials Science and Engineering, Faculty of Engineering, National University of Singapore, Singapore 117576
e-mail: msewangj@nus.edu.sg

displacive phase transition [10]. On the other hand, it is also well-known that $CaTiO_3$ exhibits an orthorhombic structure (Pcmn, D_{2h}^{16}) at $T < 1380$ K with positive harmonic soft-mode frequency. It does not undergo a ferroelectric phase transition down to $T = 0$ K, implying that the high temperature paraelectric state is always stabilized even without the suppression from quantum mechanical fluctuations [11]. By considering the difference in ferroelectric behaviours between $Pb_{0.7}La_{0.2}TiO_3$ and $CaTiO_3$, the former that exhibits soft optical phonon mode is substituted by Ca^{2+} into *A*-site to form the required stoichiometry of $Pb_{0.7(1-x)}Ca_{0.7x}La_{0.2}TiO_3$ (PCLT). In this paper, the transitions from normal ferroelectric to relaxor-like and then to quantum paraelectric-like behaviour are described and discussed for PCLT with x ranging from 0.10 to 0.60.

2 Experiment procedures

Ceramic compositions of $Pb_{0.7(1-x)}Ca_{0.7x}La_{0.2}TiO_3$ with $0 \leq x \leq 0.60$ were prepared by mechanical activation of constituent oxides for 20.0 h at room temperature, which minimizes PbO loss [12]. They exhibit a dense polycrystalline perovskite structure, upon sintering at 1150°C, as confirmed by X-ray diffraction (XRD) and scanning electron microscopy. Lattice parameters for each composition were determined from both (002) and (200) in the corresponding XRD spectrum. Room temperature Raman measurements were performed using a T64000 Jobin-Yvon triple monochromator from Horiba Inc. with the aids of 50× objective and 514.5 nm Ar^+ laser. Raman spectra at various ambient temperatures ranging from 80 to 425 K were obtained by employing a cooling stage provided by Oxford Instruments. The temperature dependences of relative permittivity (ε') of these specimens from 2.2 to 430 K were measured by HP4284A LCR meter with an a.c. voltage of 0.1 V at frequencies ranging from 100 Hz to 1 MHz. Both heating and cooling rates for the dielectric measurements are 2 K/min. A standard Sawyer-Tower circuit was employed to measure the hysteresis loops for PCLT with $0.10 \leq x \leq 0.60$ at various temperatures by applying a 10 kV/cm electric field at 1 kHz.

3 Results and discussion

Figure 1 shows the temperature dependences of (ε') for PCLT with x ranging from 0.10 to 0.60 measured at 100 kHz. Ferroelectric transitions from normal ferroelectric to relaxor-like and then to quantum paraelectric-like behaviours were observed with increasing x; however, the type of quantum ferroelectricity reported in Ca-doped $SrTiO_3$, was not observed in PCLT [6]. Both ε' maxima and transition temperature decrease with increasing x. The inset in Fig. 1 further plots

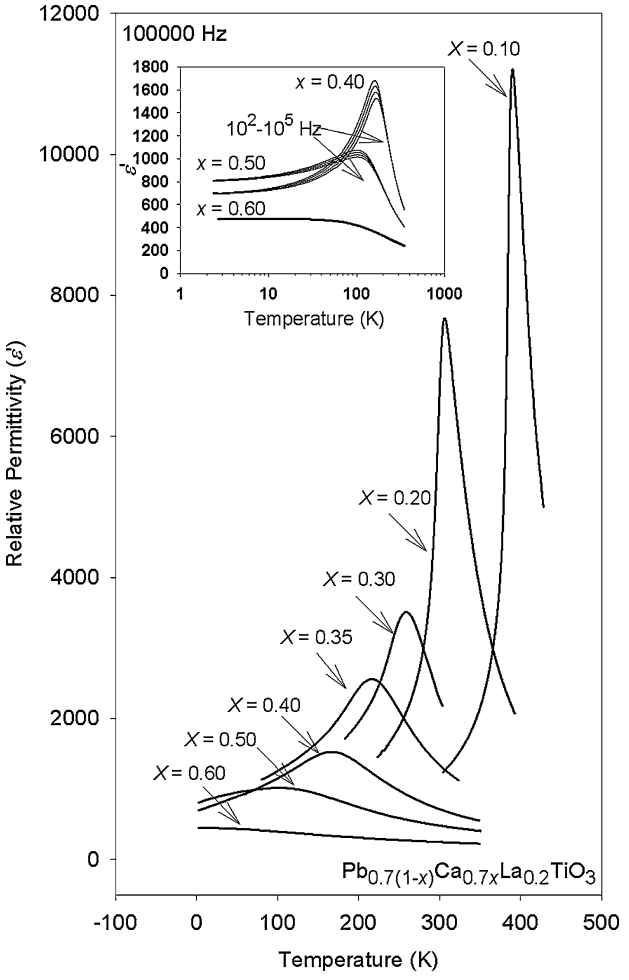

Fig. 1 Temperature dependences of relative permittivity for PCLT with $0.10 \leq x \leq 0.60$ measured at 100 kHz. The inset shows the dielectric relaxation and quantum paraelectric-like behavior for $x = 0.40$, 0.50 and 0.60, respectively

the temperature dependences of ε' for PCLT with $x = 0.40$, 0.50 and 0.60, measured at frequencies ranging from 100 Hz to 100 kHz, respectively. Frequency dispersion was observed in PCLT with $x = 0.40$ and $x = 0.50$, and then disappeared at $x = 0.60$. In addition, there occurs a thermal hysteresis for PCLT with $0.30 \leq x \leq 0.40$ that exhibits frequency dispersive relaxation, which is unusual for a typical relaxor. Figure 2 further demonstrates the compositional dependences of the Curie temperature (T_c), maximum temperature (T_{max}) and transition temperature predicted by the Barrett's relation (T_o),

$$\varepsilon' = C/[(T_1/2)\coth(T_1/2T) - T_o], \quad (1)$$

corresponding to the normal ferroelectric, relaxor-like and quantum paraelectric-like behaviour, respectively. In contrast to the crossover from the classical to quantum regime suggested by the quantum ferroelectric relation, $T_{max} \propto$

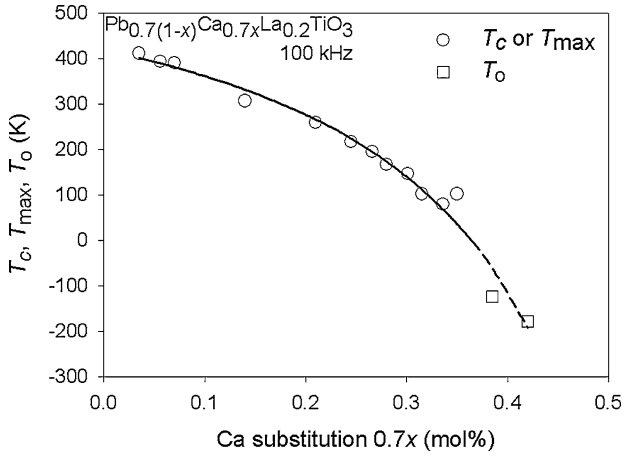

Fig. 2 Compositional dependences of transition temperatures T_c, T_{max} and T_o for PCLT. The lines are guide to the eye to transition temperatures

$(x - x_c)^{0.5}$, the compositional dependence of transition temperature for PCLT vanishes with a finite slope, i.e. dT_{max}/dx is finite when $T_{max} \rightarrow 0$ K. This is associated with the residual configuration entropy of a glassy state [13]. Thus, the relaxor-like behaviour occurs prior to the vanishing of T_{max}, such as for PCLT with $x = 0.40$, could be brought about by the condensation of non-equilibrium dipolar glass state at low temperatures, where the dipoles are frozen into random orientations. On the other hand, T_o for both PCLT with $x = 0.55$ and 0.60 are -192.5 and -196.8 K, respectively, suggesting an unattainable ferroelectric transition for these compositions.

Figure 3 shows the conventional hysteresis loops for PCLT with $x = 0.40$ measured at temperatures ranging from 2.2 to 250 K. No saturation polarization was obtained with an application of electric field up to ~15 kV/cm. Upon cooling from 250 K, the residual polarization (P_r) first increases from ~0.02 μC/cm^2 with decreasing temperatures and then becomes ~0.19 μC/cm^2 at temperature around T_{max}. The highest P_r(~0.29 μC/cm^2) was observed at ~130 K, which is 37 K below T_{max}; however further cooling to 2.2 K results in a gradual vanishing of hysteresis loop. Agreeing with the finite dT_{max}/dx demonstrated in Fig. 2, the temperature dependence of hysteresis loop for PCLT with $x = 0.40$ shows the typical characteristic of dipolar glass state, whereby P_r cannot be sustained by the dipoles frozen into random orientations. Owing to the increasing breakdown in long-range polar order, a similar temperature dependence of hysteresis loop was observed in PCLT with $0.10 \leq x \leq 0.30$, where the maximum P_r and loop area increase with decreasing x. On the other hand, upon cooling from 300 to 2.2 K, no hysteresis loop was observed for PCLT with $0.55 \leq x \leq 0.60$, which further suggests that the high temperature paraelectric state is stabilized throughout the whole temperature range for these two compositions.

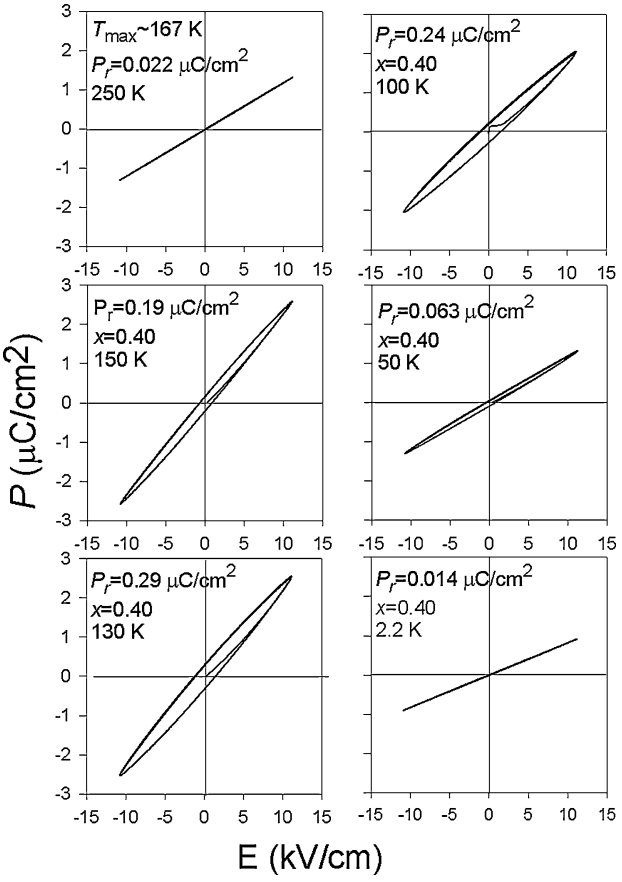

Fig. 3 Hysteresis loop for PCLT with $x = 0.40$ measured at temperatures ranging from 2.2 to 300 K

To correlate the ferroelectric behaviour with the structural parameters of PCLT, studies using XRD and micro-Raman spectroscopy were carried out. Figure 4 shows the XRD reflections for (002) and (200) for PCLT with $0.10 \leq x \leq 0.60$ measured at room temperature. Obviously, the peak splitting between (002) and (200) reflections decreases with increasing x and then become unresolved at $x = 0.60$, indicating an average cubic structure. To further quantify the change in lattice parameters, the lattice constants a and c, aspect ratio c/a and the cubic root of unit cell volume $(a^2c)^{1/3}$ are plotted as a function of x in Fig. 5(a) and (b). With increasing x from 0.10 to 0.60, the lattice parameter c decreases for ~1.2%, while the lattice parameter a decreases for only ~0.8%, resulting in the overall shrinkage of unit cell volume for ~2.8%. Thus, the shrinkage in unit cell volume can be mainly attributed to the deterioration of c-axis distortion, whereby the Pb-O hybridization in association with the lone electron pairs of Pb^{2+} is impossible for Ca^{2+} that exhibits octet electronic configuration. Moreover, the high covalency of Ca and O may also adversely affect the Ti-O hybridization, which in turn, increases the repulsion between Ti and O and favours the cubic paraelectric state [1, 2]. Microscopically, it is speculated that the decrease in transition

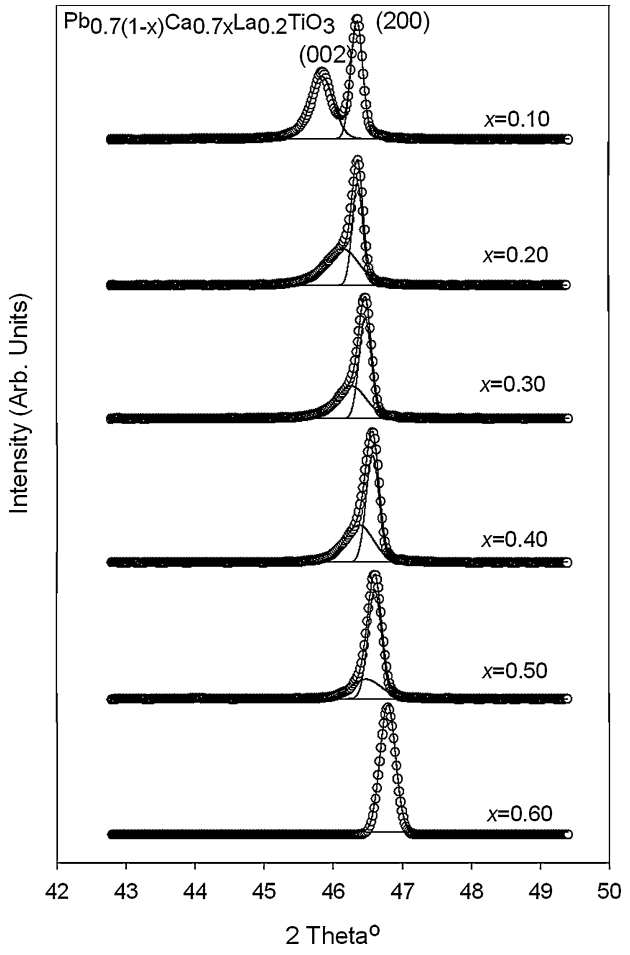

Fig. 4 XRD reflections of (002) and (200) for PCLT with $0.10 \leq x \leq 0.60$ measured at room temperature

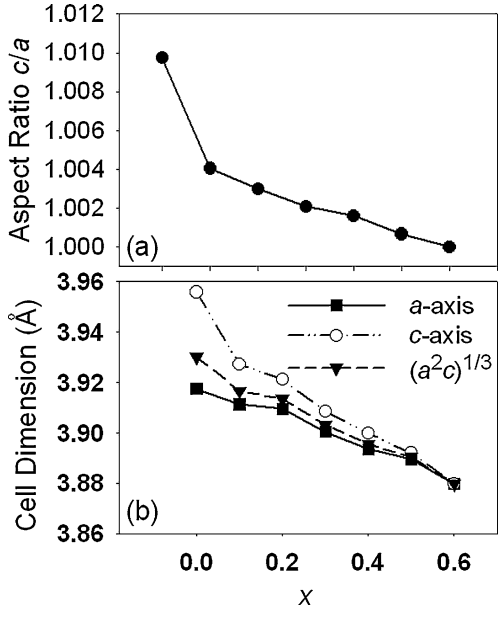

Fig. 5 (a) Aspect ratio c/a, (b) lattice parameters a, c and the cubic root of unit cell volume $(a^2c)^{1/3}$ for PCLT as a function of x

temperatures and the occurrence of quantum paraelectric-like behaviour are associated with the increasing repulsion between Ti and O. According to the soft-mode theory, the vanishing of soft-mode frequency (ω_s) at T_c is resulted by the delicate balance between the short-range repulsion and long-range Coulomb forces, which is given in terms of harmonic approximation by

$$\mu\omega_s^2 = R - [4\pi(\varepsilon_\infty + 2)(Ze^*)^2/9V], \tag{2}$$

where μ is the appropriate reduced mass, (Ze^*) is the effective ionic charge, V is the unit cell volume, ε_∞ is the high frequency dielectric constant and R is an effective short-range force constant that considers all the possible short-range repulsive forces [14]. The second term on the right represents the contribution of long-range Coulomb forces. For most of the displacive ferroelectric perovskites, the instability or phase transition is brought about by the over-cancellation of short-range repulsion by the long-range Coulomb forces, i.e. $\omega_s^2 < 0$. Since the imaginary ω_s can only be real or stabilized by anharmonic interactions, the temperature dependence of ω_s is usually given by

$$\omega_s^2 = K(T - T_c), \tag{3}$$

where K is a positive constant. With increasing x, the average unit cell volume decreases and so does the interionic distance (r) between Ti and O. Thus, ω_s^2 becomes less negative as the repulsion increases much more rapidly ($\sim r^{-10}$) than the Coulomb forces ($\sim r^{-3}$). By taking this into consideration, a lower temperature is required for stabilizing less negative ω_s^2 as suggested by Eq. (3), where an increasing x indeed reduces the transition temperature. Furthermore, a large amount of Ca^{2+} substitution ($x = 0.55$ or 0.60) can suppress the phase transition to a sufficiently low temperature regime, where the quantum mechanical fluctuations or zero-point motions become significant, leading to the quantum paraelectric-like behaviour that exhibits constant ε' over a range of temperatures.

Figure 6 plots the room temperature Raman spectra for PCLT with $0.10 \leq x \leq 0.60$, together with those of polycrystalline $PbTiO_3$ and $Pb_{0.7}La_{0.2}TiO_3$ synthesized under the same conditions. In contrast to the cubic structure suggested by XRD for PCLT with $0.30 \leq x \leq 0.60$, the asymmetric line broadening and downward shift of Raman mode frequencies suggest the breakdown in long-range polar order, which further support that the observed frequency dispersive relaxation and temperature dependence of hysteresis loop are resulted by the formation of dipolar clusters. Similar to the typical relaxor, the temperature dependence of Raman band for PCLT with $x = 0.40$ clearly indicates the existence of dipolar clusters up to ~250 K, which is substantially higher

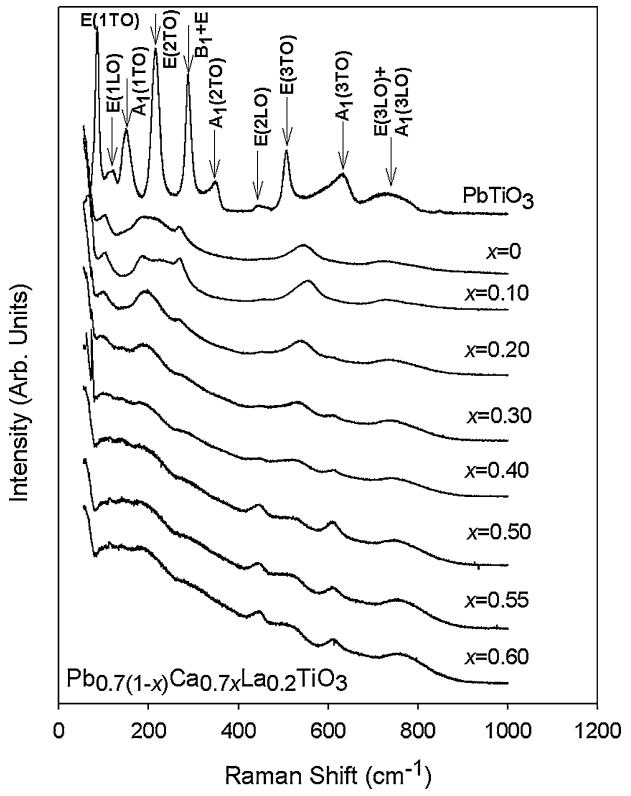

Fig. 6 Room temperature Raman spectra for PCLT with $0.10 \leq x \leq 0.60$, together with those of polycrystalline $PbTiO_3$ and $Pb_{0.7}La_{0.2}TiO_3$ synthesized under the same conditions

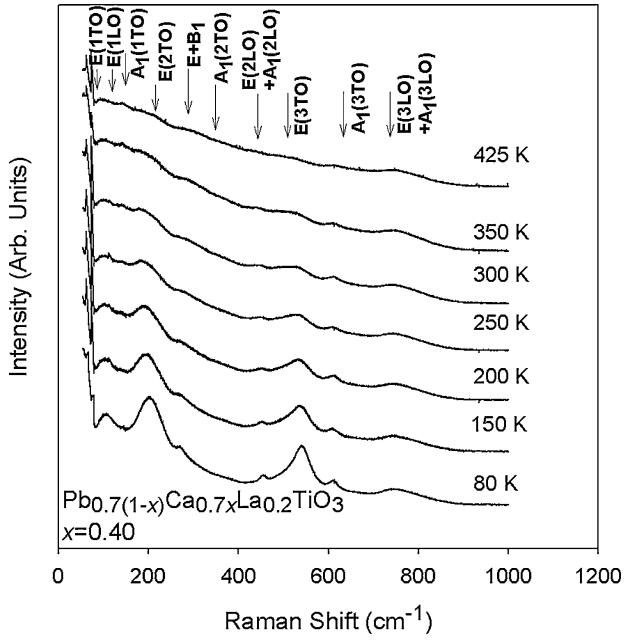

Fig. 7 Raman spectra at various temperatures for PCLT with $x = 0.40$. The positions of different Raman peaks at room temperature for polycrystalline $PbTiO_3$ synthesized under the same condition are also shown at the top

than T_{max} (~167 K), as shown in Fig. 7. Furthermore, the continuous narrowing of Raman bands with decreasing temperature shows an increase in spatial correlation length of phonon, implying that the dipolar clusters continue to grow in size upon cooling from high temperatures; however, dielectric and hysteresis loop measurements suggest that these clusters do not become large enough to permeate the whole sample (or grains) but condense into non-equilibrium dipolar glass state that exhibit dynamic slowing down fluctuations at $T \leq T_{max}$.

4 Conclusions

Transitions from ferroelectric to relaxor-like and then to quantum paraelectric-like behaviour are demonstrated by substituting Ca^{2+} into $Pb_{0.7}La_{0.2}TiO_3$. Microscopically, an increasing level of Ca^{2+} substitution stabilized the cubic paraelectric state by deteriorating Pb-O hybridization that couples the ferroelastic strain in *c*-axis of the perovskite lattice as well as increasing the repulsion between Ti and O. Indeed, both transition temperature and dielectric maxima decrease with the increasing level of Ca^{2+} substitution. By suppressing the phase transition to a sufficiently low temperature, there occurs a likelihood that the quantum paraelectric-like behavior is resulted due to the dominance of quantum mechanical fluctuations. Macroscopically, Ca^{2+} substitution results in the breakdown in long-range polar order or formation of dipolar clusters. These clusters distribute randomly into the global cubic matrix and grow in size with decreasing temperatures. Frequency dispersive dielectric relaxation associated with the slowing down dynamics of clusters was then observed for PCLT with $0.30 \leq x \leq 0.40$, which exhibits non-equilibrium dipolar glass state, as evidenced by the finite dT_{max}/dx and hysteresis loop measurements.

Acknowledgment This paper is based upon work supported by the Science and Engineering Research Council - A*Star, Singapore, under Grant No: 052 101 0047. The authors would like to thank Prof. Mitsuru Itoh and Dr. Fu Desheng of the Tokyo Institute of Technology for their assistance and discussion on the ferroelectric measurements. The support by the National University of Singapore is acknowledged.

References

1. R.E. Cohen, *Nature*, **358**, 136 (1992).
2. R.E. Cohen and H. Krakauer, *Phys. Rev. B*, **42**, 6416 (1990).
3. H. Grinberg, V.R. Cooper, and A.M. Rappe, *Nature*, **419**, 909 (2002).
4. U.T. Hochli, H.E. Weibel, and L.A. Boatner, *Phys. Rev. Lett.*, **41**, 1410 (1978).
5. J.J. van der Klink, D. Rytz, F. Borsa, and U.T. Hochli, *Phys. Rev. B*, **27**, 89 (1983).

6. J.G. Bednorz and K.A. Müller, *Phys. Rev. Lett.*, **52**, 2289 (1984).
7. H. Schremmer, W. Kleemann, and D. Rytz, *Phys. Rev. Lett.*, **62**, 1896 (1989).
8. E.L. Venturini, G.A. Samara, and W. Kleemann, *Phys. Rev. B*, **67**, 214102 (2002).
9. D. Hennings, *Mater. Res. Bull.*, **6**, 329 (1971); D. Hennings and G. Rosenstein, *Mater. Res. Bull.*, **7**, 1505 (1972).
10. B.G. Kim, S.M. Cho, T.Y. Kim, and H.M. Jang, *Phys. Rev. Lett.*, **86**, 3404 (2001); T.Y. Kim and H.Y. Jang, *Appl. Phys. Lett.*, **77**, 3824 (2000); T.Y. Kim, H.M. Jang, and S.M. Cho, *J. Appl. Phys.*, **91**, 336 (2002).
11. B.J. Kennedy, C.J. Howard, and B.C. Chakonmakos, *J. Phys.-Cond. Matt.*, **11**, 1479 (1999).
12. H.P. Soon, J.M. Xue, and J. Wang, *J. Appl. Phys.*, **95**, 4981 (2004).
13. V.V. Lemanov, E.P. Smirnova, P.P. Syrnikov, and E.A. Tarakanov, *Phys. Rev. B*, **54**, 3151 (1996).
14. G.A. Samara, T. Sakudo, and K. Yoshimitsu, *Phys. Rev. Lett.*, **35**, 1767 (1975).